Turkish Journal of Electrical Engineering & Computer Sciences

http://journals.tubitak.gov.tr/elektrik/

Research Article

Turk J Elec Eng & Comp Sci
(2013) 21: 213 – 224

doi:10.3906/elk-1106-5

A comparative study in power oscillation damping by STATCOM and SSSC based on the multiobjective PSO algorithm

Ali AJAMI[1,*], **Mehdi ARMAGHAN**[2]
[1]Electrical Engineering Department, Azarbaijan Shahid Madani University, Tabriz, Iran
[2]Young Researchers Club, Ardabil Branch, Islamic Azad University, Ardabil, Iran

Received: 01.06.2011 • **Accepted:** 01.10.2011 • **Published Online:** 27.12.2012 • **Printed:** 28.01.2013

Abstract: To improve the damping of power system oscillations by supplementary controller design for the static synchronous series compensator (SSSC) and static synchronous compensator (STATCOM), a multiobjective function based on the particle swarm optimization (PSO) algorithm for solving this optimization problem is introduced. The presented objective function includes the damping factor and the damping ratio of the lightly damped and undamped electromechanical modes. These controllers are adjusted to concurrently transfer the lightly damped and undamped electromechanical modes to a recommended region in the s-plane. For this purpose, the reduced linearized Phillips-Heffron model of the power system with a single machine and infinite bus, integrated with a STATCOM and a SSSC, is used. In this paper, to solve the mentioned optimization problem, the PSO technique is used. It is a robust stochastic optimization technique and has a high capability for discovering the most optimal results. The different loading conditions are simulated and the effects of these flexible alternating current transmission system controllers over the rotor angle and rotor speed deviations are studied. Simulation results reveal that the SSSC's performance is better than that of the STATCOM and it provides higher damping than the STATCOM. MATLAB/Simulink software is used for running the dynamic simulations.

Key words: Power system stability, particle swarm optimization, SSSC, STATCOM, multiobjective optimization

1. Introduction

Low frequency oscillations are due to large power systems being in connection together via relatively weak tie lines [1].

Using power system stabilizers (PSSs) is an effective and more economical way to moderate these power system oscillations. Because of the highly fast control action of the flexible alternating current transmission system (FACTS) devices operations, PSSs have been very favorable candidates for enhancing the damping of power system oscillations and power transfer limits [2–4]. Adding a supplementary controller to the FACTS device control system can significantly increase system damping and can also enhance the system voltage profile [3]. The static synchronous compensator (STATCOM) and static synchronous series compensator (SSSC) are 2 important members of the FACTS family. The implementation of the STATCOM and the SSSC for stability enhancement and power oscillation damping is shown in [5–9].

In this paper, using the particle swarm optimization (PSO) algorithm, the ability of the STATCOM and the SSSC supplementary controllers to improve the dynamic stability of a power system under different loading

*Correspondence: ajami@azaruniv.edu

conditions is compared. PSO is a new heuristic algorithm for global optimization searches that is based on the intelligence of swarms and social cooperation. This algorithm utilizes the swarm intelligence generated by working together and the rivalry between the particles in a swarm, and it has appeared as a practical device for engineering optimization. PSO has a pliable and properly leveled mechanism to improve the global and local exploration capabilities. It can specify the objective function and place finite bounds on the optimized parameters. It is shown in [10–15] that the PSO algorithm is a proper method for solving problems, with features such as nondifferentiability, nonlinearity, and high-dimensionality.

In [16], the imperialist competitive algorithm (ICA) was used for the tuning of damping controller parameters for a unified power flow controller. In this comparative investigation, a single machine infinite bus (SMIB) system integrated with both STATCOM and SSSC controllers is used. The multiobjective problem is in accordance with the eigenvalue-based multiobjective function, including the damping ratio and the damping factor of the lightly damped and undamped electromechanical modes. The controllers are automatically adjusted with the optimization of an eigenvalue-based multiobjective function by PSO to concurrently transfer the lightly damped and undamped electromechanical modes to a recommended region in the s-plane.

2. Description of the PSO algorithm

PSO is a new heuristic algorithm for global optimization searches that is based on the intelligence of swarms and social cooperation. It was presented for the first time in [10]. PSO uses the characteristics and behaviors of social models like bird flocking or fish training. In PSO, a swarm (a population of particles) flies over a multidimensional search space representing nominee solutions. During the search journey, current tendency, personal experience, and the swarm's experience are used to find the optimal solution [11].

The PSO algorithm requires minimal memory. It is fast, simple, and its code can be written and implemented easily. In addition to these benefits and characteristics, PSO is advantageous over evolutionary and genetic algorithms in many respects. First, PSO has memory. Unlike evolutionary programming, genetic algorithms, and evolutionary strategies, PSO does not have selection operation. PSO is the only algorithm that is not based on the survival of the fittest. PSO is based on constructive cooperation between particles. The structure of the PSO algorithm and its application in solving various problems is described in [10–15].

3. Power system modeling

3.1. Mathematical model of the power system with the STATCOM

A system with a SMIB equipped with a STATCOM is investigated, as shown in Figure 1 [5]. The STATCOM is composed of a boosting transformer, a leakage reactance $\mathbf{x_{SDT}}$, a gate turn off-based voltage source converter, and a DC link capacitor ($\mathbf{C_{DC}}$).

The STATCOM has 2 input control signals, modulation index m and phase ψ. In order to investigate the effect of the STATCOM on improving the damping of power system oscillations, its dynamic model is required. Park's transformation is applied and the resistance and transients of the transformer are neglected, and so that the STATCOM can be modeled as [5]:

$$\bar{I}_{LO} = I_{LOd} + jI_{LOq}, \tag{1}$$

$$\bar{V}_O = mkV_{DC}(\cos\psi + j\sin\psi) = mkV_{DC}\angle\psi, \tag{2}$$

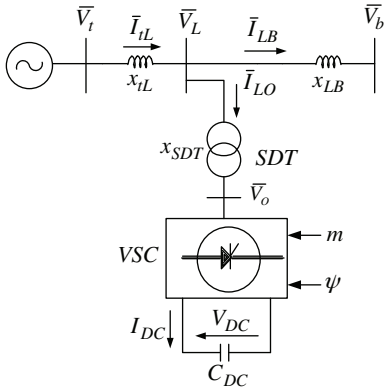

Figure 1. The system with the SMIB equipped with a STATCOM.

$$\dot{V}_{DC} = \frac{dV_{DC}}{dt} = \frac{I_{DC}}{C_{DC}}, \tag{3}$$

$$\dot{V}_{DC} = \frac{mk}{C_{DC}}(I_{LOd}\cos\psi + I_{LOq}\sin\psi). \tag{4}$$

In these equations, $\boldsymbol{k}$ is the voltage ratio between the AC and DC sides and is dependent on the inverter structure.

The nonlinear dynamic model of the presented power system in Figure 1 is [5]:

$$\dot{\delta} = \omega_b\omega, \tag{5}$$

$$\dot{\omega} = (P_m - P_e - D\omega)/M, \tag{6}$$

$$\dot{E}'_q = (-E_q + E_{fd})/T'_{do}, \tag{7}$$

$$\dot{E}_{fd} = -\frac{1}{T_A}E_{fd} + \frac{K_A}{T_A}(V_{to} - V_t), \tag{8}$$

where,

$$P_e = E'_q I_{tLq} + (x_q - x'_d)I_{tLd}I_{tLq}, E_q = E'_q + (x_d - x'_d)I_{tLd}, V_t = \sqrt{(E'_q - x'_d I_{tLd})^2 + (x_q I_{tLq})^2}.$$

By linearizing Eqs. (1) through (8), the linear dynamic model of the test power system can be obtained as follows [5]:

$$\Delta\dot{\delta} = \omega_b\Delta\omega, \tag{9}$$

$$\Delta\dot{\omega} = (-\Delta P_e - D\Delta\omega)/M, \tag{10}$$

$$\Delta\dot{E}'_q = (-\Delta E_q + \Delta E_{fd})/T'_{do}, \tag{11}$$

$$\Delta\dot{E}_{fd} = -\frac{1}{T_A}\Delta E_{fd} - \frac{K_A}{T_A}\Delta V_t, \tag{12}$$

$$\Delta\dot{V}_{DC} = K_7\Delta\delta + K_8\Delta E'_q + K_9\Delta V_{DC} + K_{dm}\Delta m + K_{d\psi}\Delta\psi, \tag{13}$$

where,

$$\Delta P_e = K_1\Delta\delta + K_2\Delta E'_q + K_{pDC}\Delta V_{DC} + K_{pm}\Delta m + K_{p\psi}\Delta\psi,$$

$$\Delta E_q = K_4\Delta\delta + K_3\Delta E'_q + K_{qDC}\Delta V_{DC} + K_{qm}\Delta m + K_{q\psi}\Delta\psi,$$

$$\Delta V_t = K_5\Delta\delta + K_6\Delta E'_q + K_{vDC}\Delta V_{DC} + K_{vm}\Delta m + K_{v\psi}\Delta\psi.$$

$\boldsymbol{K_1}$, $\boldsymbol{K_2}$, ..., $\boldsymbol{K_9}$,$\boldsymbol{K_{pu}}$, $\boldsymbol{K_{qu}}$, $\boldsymbol{K_{du}}$, and $\boldsymbol{K_{vu}}$ are linearization coefficients that are dependent on the operating conditions and system parameters. Finally, the state space equations of the test power system can be obtained as below:

$$\dot{x} = Ax + Bu, \tag{14}$$

where the state matrix $\boldsymbol{A}$, input matrix $\boldsymbol{B}$, state variables vector $\boldsymbol{x}$, and control input vector $\boldsymbol{u}$ are:

$$x = \begin{bmatrix} \Delta\delta & \Delta\omega & \Delta E'_q & \Delta E_{fd} & \Delta V_{DC} \end{bmatrix}^T, u = \begin{bmatrix} \Delta m & \Delta\psi \end{bmatrix}^T,$$

$$A = \begin{bmatrix} 0 & \omega_b & 0 & 0 & 0 \\ -\frac{K_1}{M} & -\frac{D}{M} & -\frac{K_2}{M} & 0 & -\frac{K_{pDC}}{M} \\ -\frac{K_4}{T'_{do}} & 0 & -\frac{K_3}{T'_{do}} & \frac{1}{T'_{do}} & -\frac{K_{qDC}}{T'_{do}} \\ -\frac{K_A K_5}{T_A} & 0 & -\frac{K_A K_6}{T_A} & -\frac{1}{T_A} & -\frac{K_A K_{vDC}}{T_A} \\ K_7 & 0 & K_8 & 0 & K_9 \end{bmatrix}, \quad B = \begin{bmatrix} 0 & 0 \\ -\frac{K_{pm}}{M} & -\frac{K_{p\psi}}{M} \\ -\frac{K_{qm}}{T'_{do}} & -\frac{K_{q\psi}}{T'_{do}} \\ -\frac{K_A K_{vm}}{T_A} & -\frac{K_A K_{v\psi}}{T_A} \\ K_{dm} & K_{d\psi} \end{bmatrix}.$$

Figure 2 shows the block diagram of the linearized dynamic model of the test system.

3.2. Mathematical model of the power system with the SSSC

The SSSC modeling is performed similar to the STATCOM modeling. A system with a SMIB equipped with SSSC is investigated, as shown in Figure 3 [8]. The SSSC typically has the same power electronics topology as the STATCOM. However, it is combined into the AC power system through a series coupling transformer, in contrast to the shunt transformer in the STATCOM. The dynamic model of the SSSC can be modeled as [8]:

$$\bar{I}_{tL} = I_{tLd} + jI_{tLq} = I_{TL}\angle\phi, \tag{15}$$

$$\begin{array}{l} \bar{V}_{INV} = mkV_{DC}(\cos\psi + j\sin\psi) = mkV_{DC}\angle\psi \\ \psi = \phi \pm 90^o \end{array}, \tag{16}$$

$$\dot{V}_{DC} = \frac{dV_{DC}}{dt} = \frac{I_{DC}}{C_{DC}}, \tag{17}$$

$$\dot{V}_{DC} = \frac{mk}{C_{DC}}(I_{tLd}\cos\psi + I_{tLq}\sin\psi). \tag{18}$$

In these equations, $\boldsymbol{k}$ is the voltage ratio between the AC and DC sides and is dependent on the inverter structure.

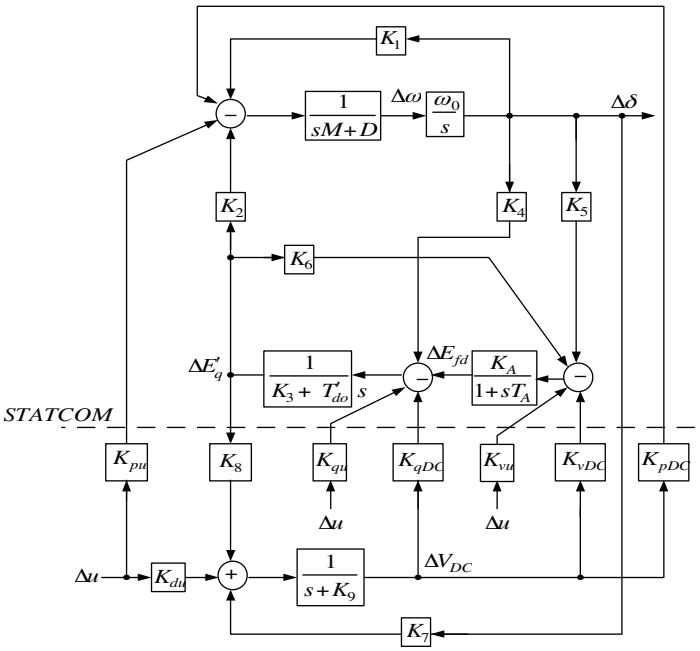

Figure 2. Reduced linearized Phillips-Heffron model of a SMIB system integrated with the STATCOM.

The nonlinear dynamic model of the power system in Figure 3 is [8]:

$$\dot{\delta} = \omega_b \omega, \tag{19}$$

$$\dot{\omega} = (P_m - P_e - D\omega)/M, \tag{20}$$

$$\dot{E}'_q = (-E_q + E_{fd})/T'_{do}, \tag{21}$$

$$\dot{E}_{fd} = -\frac{1}{T_A} E_{fd} + \frac{K_A}{T_A}(V_{to} - V_t), \tag{22}$$

where,

$$P_e = E'_q I_{tLq} + (x_q - x'_d) I_{tLd} I_{tLq}, E_q = E'_q + (x_d - x'_d) I_{tLd}, V_t = \sqrt{(E'_q - x'_d I_{tLd})^2 + (x_q I_{tLq})^2}.$$

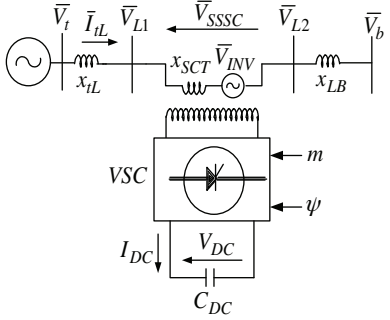

Figure 3. The system with a SMIB equipped with SSSC.

By linearizing Eqs. (15) through (22), a linear dynamic model of the test power system equipped with a SSSC can be obtained as [8]:

$$\Delta\dot{\delta} = \omega_b \Delta\omega, \tag{23}$$

$$\Delta\dot{\omega} = (-\Delta P_e - D\Delta\omega)/M, \tag{24}$$

$$\Delta\dot{E'}_q = (-\Delta E_q + \Delta E_{fd})/T'_{do}, \tag{25}$$

$$\Delta\dot{E}_{fd} = -\frac{1}{T_A}\Delta E_{fd} - \frac{K_A}{T_A}\Delta V_t, \tag{26}$$

$$\Delta\dot{V}_{DC} = K'_7\Delta\delta + K'_8\Delta E'_q + K'_9\Delta V_{DC} + K'_{dm}\Delta m + K'_{d\psi}\Delta\psi, \tag{27}$$

where,

$$\Delta P_e = K'_1\Delta\delta + K'_2\Delta E'_q + K'_{pDC}\Delta V_{DC} + K'_{pm}\Delta m + K'_{p\psi}\Delta\psi,$$

$$\Delta E_q = K'_4\Delta\delta + K'_3\Delta E'_q + K'_{qDC}\Delta V_{DC} + K'_{qm}\Delta m + K'_{q\psi}\Delta\psi,$$

$$\Delta V_t = K'_5\Delta\delta + K'_6\Delta E'_q + K'_{vDC}\Delta V_{DC} + K'_{vm}\Delta m + K'_{v\psi}\Delta\psi.$$

$\boldsymbol{K'_1}, \boldsymbol{K'_2}, \ldots, \boldsymbol{K'_9}, \boldsymbol{K'_{pu}}, \boldsymbol{K'_{qu}}, \boldsymbol{K'_{du}}$, and $\boldsymbol{K'_{vu}}$ are linearization coefficients and are dependent on the operating conditions and system parameters. Finally, the state space model of the test power system can be given as:

$$\dot{x} = Ax + Bu, \tag{28}$$

where the state matrix $\boldsymbol{A}$, input matrix $\boldsymbol{B}$, state variables vector $\boldsymbol{x}$, and control input vector $\boldsymbol{u}$ are:

$$x = \begin{bmatrix} \Delta\delta & \Delta\omega & \Delta E'_q & \Delta E_{fd} & \Delta V_{DC} \end{bmatrix}^T, u = \begin{bmatrix} \Delta m & \Delta\psi \end{bmatrix}^T,$$

$$A = \begin{bmatrix} 0 & \omega_b & 0 & 0 & 0 \\ -\frac{K'_1}{M} & -\frac{D}{M} & -\frac{K'_2}{M} & 0 & -\frac{K'_{pDC}}{M} \\ -\frac{K'_4}{T'_{do}} & 0 & -\frac{K'_3}{T'_{do}} & \frac{1}{T'_{do}} & -\frac{K'_{qDC}}{T'_{do}} \\ -\frac{K_A K'_5}{T_A} & 0 & -\frac{K_A K'_6}{T_A} & -\frac{1}{T_A} & -\frac{K_A K'_{vDC}}{T_A} \\ K'_7 & 0 & K'_8 & 0 & K'_9 \end{bmatrix}, \quad B = \begin{bmatrix} 0 & 0 \\ -\frac{K'_{pm}}{M} & -\frac{K'_{p\psi}}{M} \\ -\frac{K'_{qm}}{T'_{do}} & -\frac{K'_{q\psi}}{T'_{do}} \\ -\frac{K_A K'_{vm}}{T_A} & -\frac{K_A K'_{v\psi}}{T_A} \\ K'_{dm} & K'_{d\psi} \end{bmatrix}.$$

Figure 4 shows the block diagram of the linearized dynamic model of the test system.

3.3. Power system oscillation damping controller

The damping controller shown in Figure 5 is provided to enhance the damping of the power system oscillations. This controller includes gain block, signal-washout block, and a lead–lag compensator, and is used for the STATCOM and the SSSC [3].

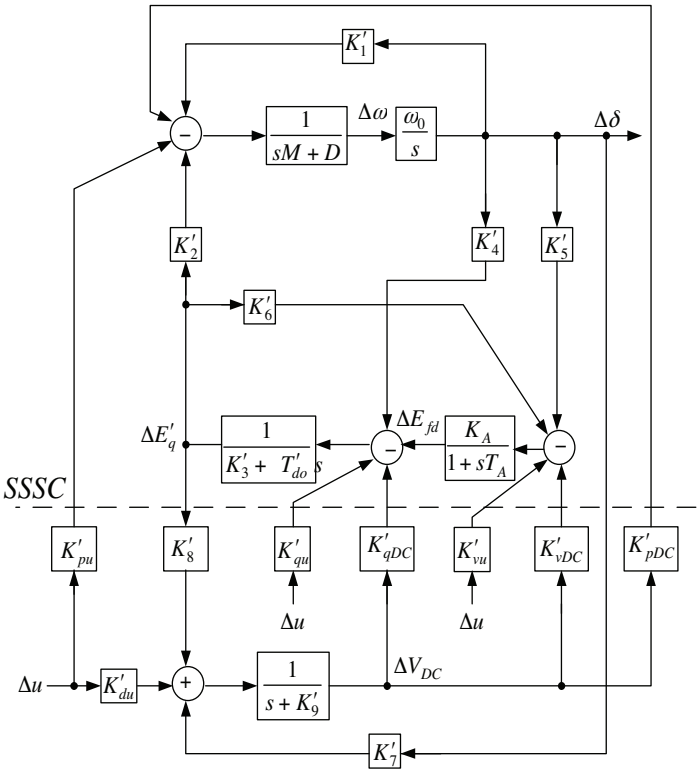

Figure 4. Reduced linearized Phillips-Heffron model of the SMIB system integrated with a SSSC.

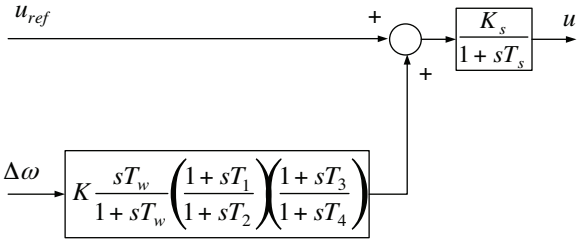

Figure 5. STATCOM/SSSC with a lead–lag controller.

3.4. Optimization problem

In this paper, to enhance the overall system dynamic stability under different operating conditions, the STATCOM and SSSC controller parameters are optimally tuned. For this purpose, an eigenvalue-based multiobjective function including the damping ratio and the damping factor is considered as follows [17,18]:

$$J_3 = J_1 + aJ_2, \tag{29}$$

where $J_1 = \sum_{\sigma_i \geq \sigma_0} (\sigma_0 - \sigma_i)^2$, $J_2 = \sum_{\zeta_i \leq \zeta_0} (\zeta_0 - \zeta_i)^2$, $\sigma_{\mathbf{i}}$, and $\zeta_{\mathbf{i}}$ are the real part and the damping ratio of the $\boldsymbol{i}$th eigenvalue, respectively. The value of term **a** is selected as 10 and it is a weighting coefficient for combining both damping factors and damping ratios. The relative stability in terms of the damping factor margin is determined by $\sigma_{\mathbf{0}}$. When only $\mathbf{J_1}$ is considered as the objective function, according to Figure 6a, the closed-loop eigenvalues are placed in the region to the left of the dashed line. Similarly, when only $\mathbf{J_2}$ is taken, the closed-loop eigenvalues are placed in the region that is shown in Figure 6b. In this case, $\zeta_{\mathbf{0}}$ is the

optimal damping ratio that is to be obtained. If $\mathbf{J_3}$ is taken as the objective function, according to Figure 6c, the eigenvalues are limited within a D-shaped area.

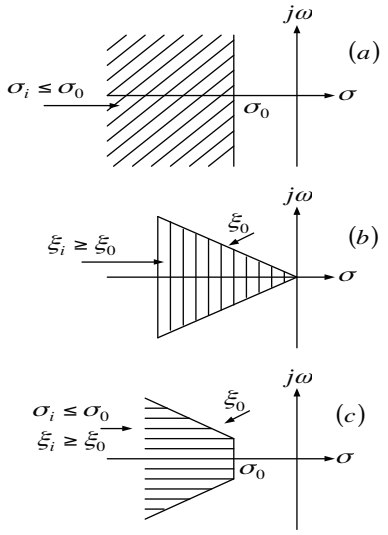

Figure 6. Region of the eigenvalue location for the objective functions.

The minimization of $\mathbf{J_3}$ is our optimization problem subject to:

$$\min \leq K, T_1, T_2, T_3, T_4 \leq \max . \tag{30}$$

In this paper, the range of $\boldsymbol{K}$ is taken as [0.01–100] and [0.01–1], and it is determined for $\boldsymbol{T_1}$, $\boldsymbol{T_2}$, $\boldsymbol{T_3}$, and $\boldsymbol{T_4}$.

In the suggested method, the PSO algorithm is used to solve this optimization problem and to search for the optimal set of STATCOM and SSSC damping controller parameters. In this paper, the values of σ_0 and ζ_0 are taken as –1.5 and 0.2, respectively. Moreover, in this simulation, the PSO algorithm parameters are considered as follows: the number of particles = 30, particle size = 5, number of iterations = 50, c1 = 2, and c2 = 2. Furthermore, the inertia weight, w, is linearly decreasing from 0.9 to 0.4.

4. Simulation results

The SMIB test system, integrated with a STATCOM and a SSSC as shown in Figures 1 and 3, respectively, is considered for simulation studies. The performance of the suggested controller for the SSSC and STATCOM during transient conditions is verified by applying a 3-phase fault at t = 1 s, at the infinite bus. The response of the system that is presented in this case and for different loading conditions is given in Table 1 and the abilities of the SSSC and STATCOM in low-frequency oscillation damping are compared.

The optimized values of the supplementary controller parameters based on multiobjective function $\mathbf{J_3}$ in the 3 loading conditions for the STATCOM and the SSSC are given in Table 2.

The results of the rotor angle deviation and rotor speed deviation under light, nominal, and heavy loading conditions are shown in Figures 7, 8, and 9, respectively. These show that the PSO-based SSSC controller tuned using the multiobjective function acts better than the STATCOM controller and greatly improves the dynamic stability of the power system.

Table 1. Loading conditions.

Loading	P (pu)	Q (pu)
Nominal	0.9	0.08
Light	0.65	0.15
Heavy	1.2	0.12

Table 2. The optimal parameters of the proposed controllers.

Controller parameters	STATCOM			SSSC		
	Light	Nominal	Heavy	Light	Nominal	Heavy
K	90.3866	71.8420	40.2062	87.0085	67.9471	100
T_1	0.8954	0.6484	0.8023	1	0.7257	0.1515
T_2	0.4363	0.3113	0.4723	0.1329	0.0838	0.0100
T_3	0.7029	0.7426	1	0.7388	1	0.9988
T_4	0.2385	0.2300	0.1571	0.1872	0.2589	0.2192

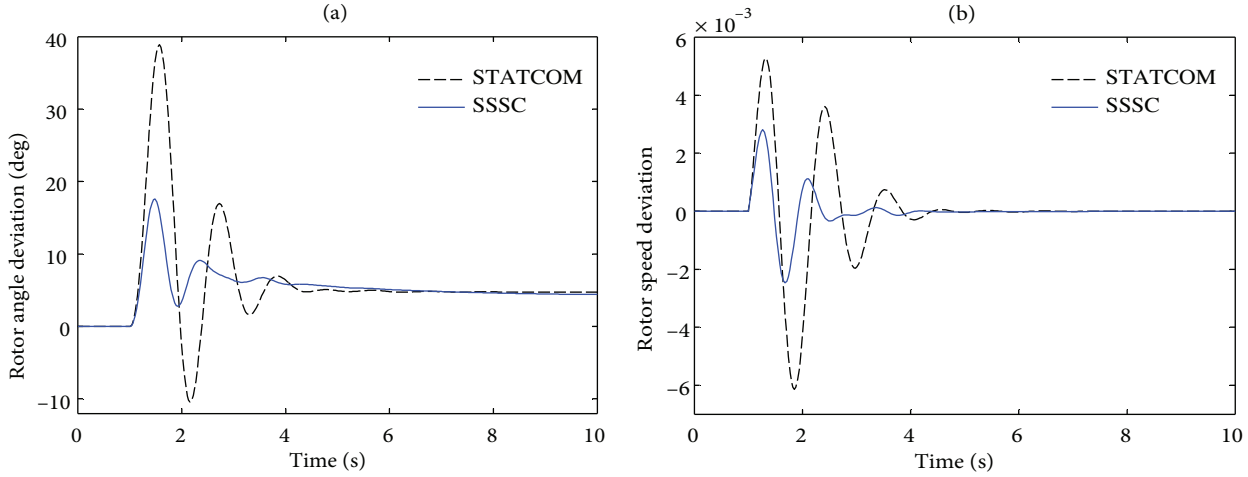

Figure 7. Dynamic responses for a) rotor angle deviation and b) rotor speed deviation under light loading conditions.

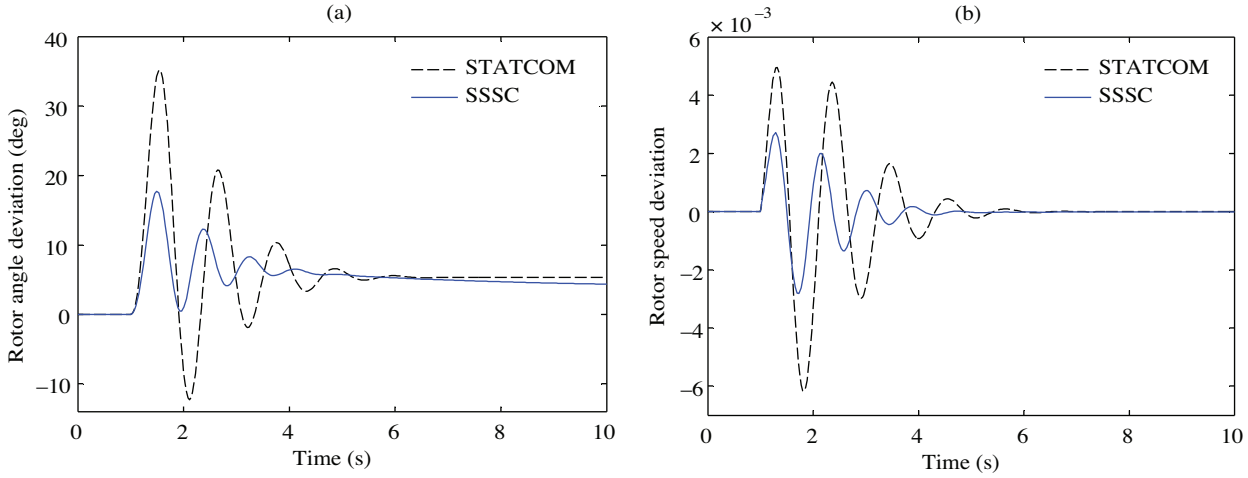

Figure 8. Dynamic responses for a) rotor angle deviation and b) rotor speed deviation under nominal loading conditions.

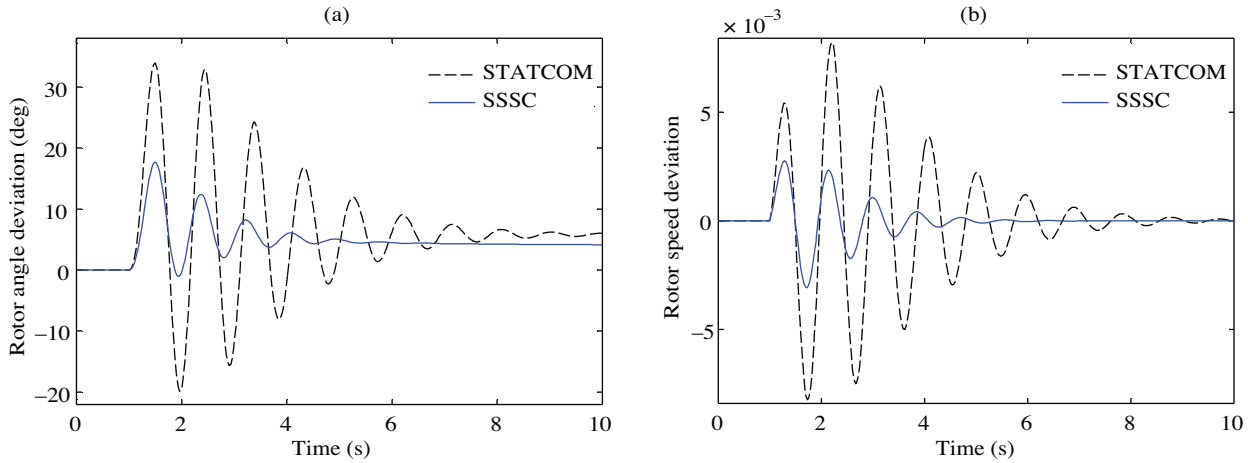

Figure 9. Dynamic responses for a) rotor angle deviation and b) rotor speed deviation under heavy loading conditions.

In this section, we present a comparison of the current results with those of other published papers on this subject. In [19], a neural network-based intelligent control for improving the dynamic performance of FACTS devices was presented. Figure 10 shows the results of the rotor angle δ, where the curves of the SSSC, conventional external linear controller (CONVEC), and indirect adaptive external neurocontroller (INDAEC) indicate the system response without the supplementary oscillation damping controller, conventional controller, and radial basis function neural network-based INDAEC applied to the SSSC, respectively. These results clearly show that the damping control of the low-frequency power oscillations by the INDAEC is much better than that of the SSSC and the CONVEC.

In [20], a nonlinear control design series of FACTS devices for damping power system oscillations was presented. Figure 11 shows the rotor angle of the generator with and without a SSSC when a 3-phase fault occurs. In this Figure, K is the gain of the oscillation damping controller.

In [21], a static shunt and the series compensations of a SMIB system using a flying capacitor multilevel inverter were presented. Figure 12 shows the rotor speed deviation for the uncompensated system and compensated system with a STATCOM and a SSSC.

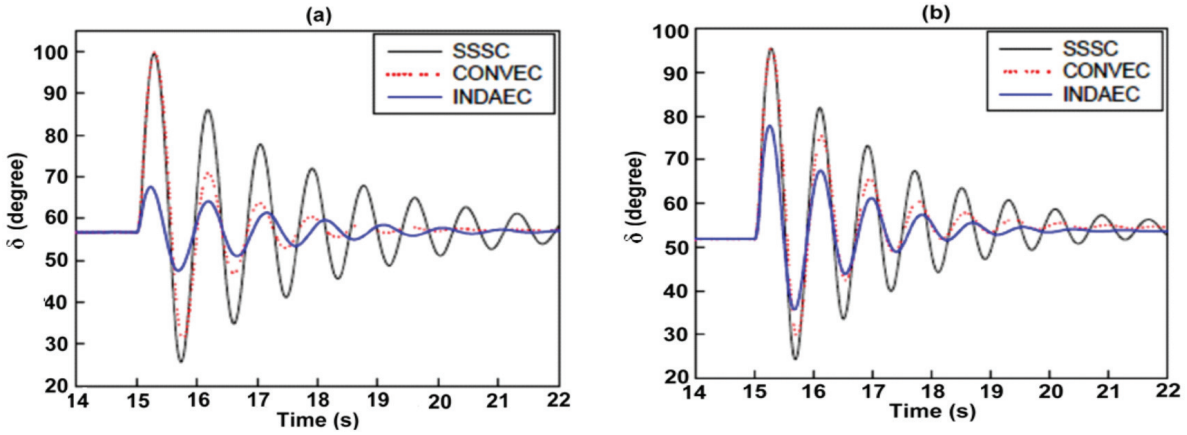

Figure 10. Dynamic responses of the rotor angle when a 3-phase fault occurs at a) P = 0.8 pu, Q = 0.12 pu and b) P = 0.88 pu, Q = 0.22 pu [19].

It can be observed that the SSSC is more effective in damping the oscillations than the STATCOM.

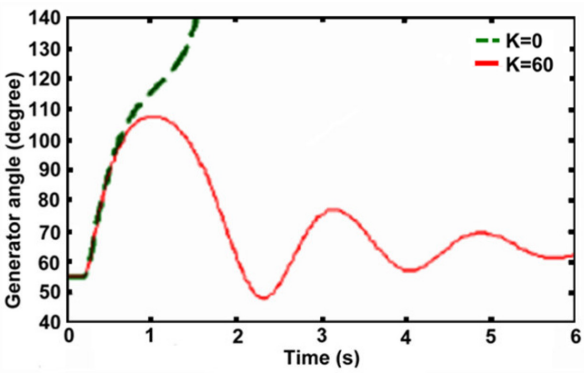

Figure 11. The generator rotor angle of the system with (K = 60) and without (K = 0) a SSSC [20].

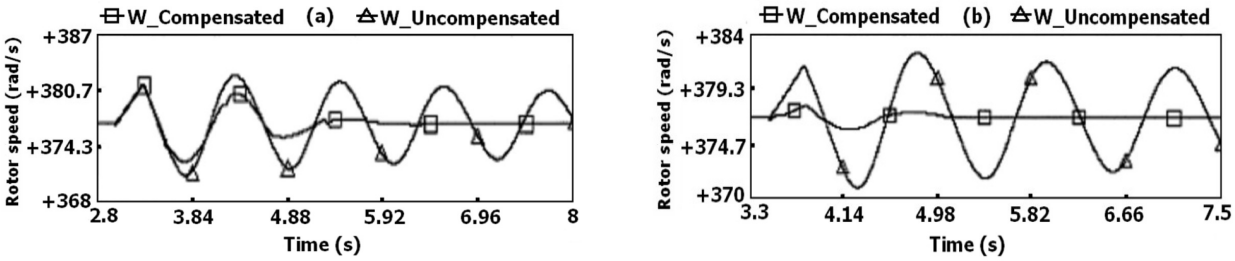

Figure 12. Rotor speed oscillation (in radians per second) in the compensated system with a) a STATCOM and b) a SSSC [21].

Comparing Figures 7–12, it can be seen that the presented method in this paper is better and has a fast response in oscillation damping.

5. Conclusion

The STATCOM and the SSSC are important FACTS devices. This paper presents a PSO-based power oscillation damping controller for a SMIB integrated with a STATCOM and a SSSC. Their performance comparison in terms of transient stability enhancement and oscillations damping is presented. The stabilizer is adjusted concurrently to transfer the lightly damped and undamped electromechanical modes of the machine to a recommended region in the s-plane. The presented objective function includes the damping factor and the damping ratio of the lightly damped and undamped electromechanical modes. The simulation results reveal that both the STATCOM and the SSSC can significantly enhance the damping of oscillation and guarantee the stability of the system. It also reveals that the SSSC performance is better than that of the STATCOM, and it provides higher damping than the STATCOM.

Appendix

The test systems parameters are:

Machine: $D = 0$; $x_d = 1$; $x_q = 0.6$; $x_d^{'} = 0.3$; $M = 8$; $T_{do}^{'} = 5.044$; $f = 60$; $V_t = 1$.

Excitation system: $K_A = 120$; $T_A = 0.05$.

Transmission line: $x_{tL} = 0.15$; $x_{LB} = 0.6$.

STATCOM: $C_{DC} = 1$; $V_{DC} = 2$; $K_s = 1.2$; $T_s = 0.05$; $T_w = 0.01$; $x_{SDT} = 0.15$.

SSSC: $C_{DC} = 0.25$; $V_{DC} = 1$; $K_s = 1.2$; $T_s = 0.05$; $T_w = 0.01$; $x_{SCT} = 0.15$.

References

[1] P. Kundur, Power System Stability and Control, New York, McGraw-Hill, 1994.

[2] A.J.F. Keri, A.S. Mehraban, X. Lombard, A. Eiriachy, A.A. Edris, "Unified power flow controller (UPFC): modeling and analysis", IEEE Transactions on Power Delivery, Vol. 14, pp. 648–654, 1999.

[3] H. Shayeghi, H.A. Shayanfar, S. Jalilzadeh, A. Safari, "A PSO based unified power flow controller for damping of power system oscillations", Energy Conversion and Management, Vol. 50, pp. 2583–2592, 2009.

[4] A.T. Al-Awami, Y.L. Abdel-Magid, M.A. Abido, "A particle swarm-based approach of power system stability enhancement with unified power flow controller", International Journal of Electrical Power and Energy Systems, Vol. 29, pp. 251–259, 2007.

[5] H.F. Wang, "Phillips-Heffron model of power systems installed with STATCOM and applications", IEE Proceedings - Generation, Transmission and Distribution, Vol. 146, pp. 521–527, 1999.

[6] L. Gyugyi, C.D. Schauder, K.K. Sen, "Static synchronous series compensator: a solid-state approach to the series compensation of transmission lines", IEEE Transactions on Power Delivery, Vol. 12, pp. 406–417, 1997.

[7] H.F. Wang, "Static synchronous series compensator to damp power system oscillations", Electric Power Systems Research, Vol. 54, pp. 113–119, 2000.

[8] H.F. Wang, "Design of SSSC damping controller to improve power system oscillation stability", IEEE Africon, Vol. 1, pp. 495–500, 1999.

[9] N.G. Hingorani, L. Gyugyi, Understanding FACTS: Concepts and Technology of Flexible AC Transmission Systems, New Jersey, Wiley-IEEE Press, 1999.

[10] J. Kennedy, R. Eberhart, "Particle swarm optimization", Proceedings of the IEEE International Conference on Neural Networks, Vol. 4, pp. 1942–1948, 1995.

[11] A.Z. Şevkli, F.E. Sevilgen, "StPSO: strengthened particle swarm optimization", Turkish Journal of Electrical Engineering & Computer Sciences, Vol. 18, pp. 1095–1114, 2010.

[12] R. Eberhart, J. Kennedy, "A new optimizer using particle swarm theory", Proceedings of the 6th International Symposium on Micro Machine and Human Science, pp. 39–43, 1995.

[13] R. Eberhart, J. Kennedy, Y. Shi, Swarm Intelligence, San Francisco, Morgan Kaufmann Publishers, 2001.

[14] Z.L. Gaing, "A particle swarm optimization approach for optimum design of PID controller in AVR system", IEEE Transaction on Energy Conversions, Vol. 9, pp. 384–391, 2004.

[15] M. Clerc, J. Kennedy, "The particle swarm-explosion, stability, and convergence in a multidimensional complex space", IEEE Transactions on Evolutionary Computation, Vol. 6, pp. 58–73, 2002.

[16] A. Ajami, R. Gholizadeh, "Optimal design of UPFC-based damping controller using imperialist competitive algorithm", Turkish Journal of Electrical Engineering & Computer Sciences, Vol. 20, pp. 1109–1122, 2012.

[17] Y.L. Abdel-Magid, M.A. Abido, "Optimal multiobjective design of robust power system stabilizers using genetic algorithms", IEEE Transaction on Power Systems, Vol. 18, pp. 1125–1132, 2003.

[18] M.A. Abido, Y.L. Abdel-Magid, "Optimal design of power system stabilizers using evolutionary programming", IEEE Transactions on Energy Conversion, Vol. 17, pp. 429–436, 2002.

[19] Q. Wei, R.G. Harley, G.K. Venayagamoorthy, "Neural-network–based intelligent control for improving dynamic performance of FACTS devices", IREP Symposium - Bulk Power System Dynamics and Control - VII Revitalizing Operational Reliability, pp. 1–9, 2007.

[20] P. Kumkratug, "Nonlinear control design of series FACTS devices for damping power system oscillation", American Journal of Applied Sciences, Vol. 8, pp. 124–128, 2011.

[21] A. Shukla, A. Ghosh, A. Joshi, "Static shunt and series compensations of an SMIB system using flying capacitor multilevel inverter", IEEE Transactions on Power Delivery, Vol. 20, pp. 2613–2622, 2005.